3D airborne electromagnetic inversion using a hybrid edge-based FE-IE method with moving sensitivity domain

Leif H. Cox, TechnoImaging, and Michael S. Zhdanov, University of Utah and TechnoImaging

Summary

This paper introduces an approach to 3D modeling and inversion of the airborne electromagnetics (AEM) that is suited to arbitrarily complex earth models with very high conductivity contrasts and rugged topography, yet is fast enough to consider large surveys. We use a hybrid FE-IE method, which directly avoids errors associated with numerical differentiation and interpolation of the electric vector potentials at the edges of the elements containing the receiver. This approach is stable and accurate and for conductivity contrasts in excess of 10^8:1, as is typically required for practical AEM interpretation. We incorporate the moving sensitivity domain method into this modeling framework to increase the modeling speed for an entire survey by several orders of magnitude. A case study for the 3D inversion of 90 line km of DIGHEM data from the Reid-Mahaffy test site is presented to demonstrate the efficacy of our method.

Introduction

Cox and Zhdanov (2007) and Cox et al. (2010, 2012) introduced the 3D inversion of entire AEM surveys using a moving sensitivity domain methodology. Their modeling was based on a frequency-domain contraction integral equation (IE) method (Hursán and Zhdanov, 2002; Zhdanov, 2002, 2009) that solved for the total electric field while preserving a distributed source term. Time-domain AEM responses and sensitivities were evaluated by a cosine transform and convolution with the transmitter waveform (e.g., Raiche, 1998). While this has proven to be very versatile in practice, in some circumstances, it may be advantageous to use an alternative modeling method. One obvious candidate would be the compact finite-element (CFE) method which couples the geometric flexibility of the finite-element (FE) method with the limited domain of the integral equation method (e.g., Gupta et al., 1989; Raiche and Sugeng, 1989; Ellis, 1999; Raiche et al., 2007). However, CFE methods are inefficient to implement in a moving sensitivity domain inversion because the hybrid FE-IE system matrix needs to be reconstructed for each sensitivity domain.

Alternatively, one may consider finite-element (FE) methods which differ from IE and CFE methods in two important aspects. First, the fields must be solved everywhere on a grid above and within the earth to simulate an unbound medium, rather than just within the volume of interest. Second, the resultant matrix system is sparse and diagonally banded. The sparsity allows larger domains, while the flexible gridding inherent in the FE method permits cells to grow rapidly near the boundary minimizing the impact of the simulated unbounded domain.

Our implementation of the FE method follows that of Sugeng (1998) and Sugeng and Raiche (2004). This method directly avoids errors associated with numerical differentiation and interpolation of the electric vector potentials at the edges of the element containing the receiver, which is essentially a hybrid FE-IE method that retains many of the advantages of both methods. The mesh generation is based on a moving sensitivity domain approach, which allows the domain size for forward modeling and sensitivity calculations to remain small relative to the entire domain of interest.

We apply the developed hybrid FE–IE moving sensitivity domain method to AEM frequency domain field data collected at the Ried-Mahaffy test site in Ontario, Canada. These results are compared against the results based on the integral equations code of Cox et al. (2012).

Modeling methodology

The forward modeling method uses a secondary field formulation with the total field being decomposed into a primary (background) field and secondary (anomalous) field. Following Sugeng and Raiche (2004), we chose the background conductivity as a homogenous whole space of low but finite conductivity. In this case, the background fields and domain-to-receiver Green's functions used to evaluate the response are given by analytic solutions, which speed up computation significantly.

The 3D heterogeneous domain is divided into a 3D mesh with eight nodes per iso-parametric element. The use of the linear vector basis and test functions results in twelve unknown parameters per element; those being the tangential electric vector potentials at the midpoint of each edge of the element. The shape functions are derived to ensure the continuity of the tangential and perpendicular electric vector potentials at the element boundaries (e.g., Mur, 1994; Silvester and Ferrari, 1996).

Since each element interacts with the elements in its immediate neighborhood only, the stiffness matrix is sparse. The small bandwidth is preserved by using

DOI http://dx.doi.org/10.1190/segam2014-0927.1

homogeneous Dirichlet boundary conditions. The extra discretization required for this far-field representation does not present a significant computational overhead since the iso-parametric FE method allows for considerable independence in the lateral and depth spacing of these nodes.

In the framework of the moving sensitivity domain approach, we first consider the mesh as for a single sounding location. The mesh is centered on a transmitter-receiver pair, and the center of the mesh is uniformly discretized in the horizontal directions to facilitate the inversion (Figure 1). This is referred to as the sensitivity domain. Outside of this region, cells increase in size to create an intermediate padding region. The conductivity variations in this region are considered and this area is termed the variable conductivity domain. Beyond this region are a small number of very large scale cells which comprise a padding region to enforce the homogenous boundary conditions. The conductivity in this region is set as some background conductivity and does not vary laterally or during inversion.

For multiple sounding locations, the mesh is recycled and each transmitter-receiver pair remains above the center of the mesh. The conductivity structure in the area of interest is effectively laterally translated through the mesh until the entire survey is modeled. Since the linear system for each sensitivity domain is different, it is more efficient to use iterative solvers than direct ones. For the relatively small

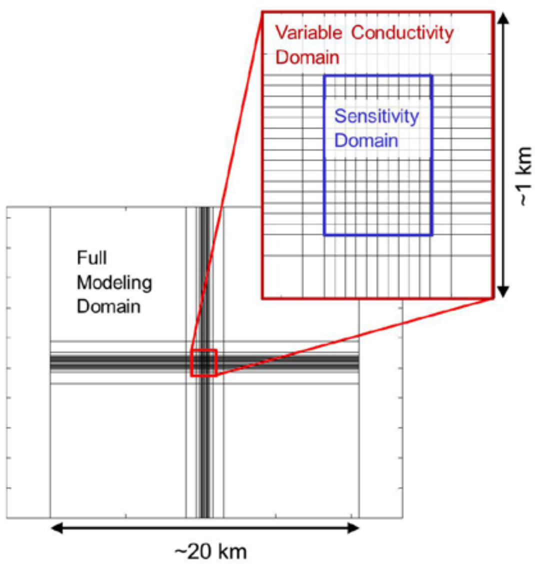

Figure 1: A schematic of the meshing in map view. The figure on the lower left shows the entire modeling domain. The insert shows a close-up of the center of the modeling domain.

number of edges (i.e., unknowns) in each sensitivity domain, the computational cost for iterative solvers is quite low.

Verification

We have verified the accuracy of the FE modeling by comparison with an independent method. The second method is the high contrast integral equation method with bilinear basis functions as developed by Farquharson (2006). The synthetic model is 1 Ohm-m body embedded in a 1000 Ohm-m half space. The body is cubic with dimensions 50 m in each direction and the depth to top is 25 m. A frequency domain flight line at 1000 Hz with a coplanar configuration was synthesized over the center of the body. The inphase and quadrature response for both methods are shown in Figure 2. The two methods are completely independent and show excellent agreement for the 1000:1 contrast within the modeling domain. In addition, the background conductivity for the FE method is a resistive whole space, implying the maximum contrast in the model is 1E8, further verifying the accuracy of the solution at high contrast.

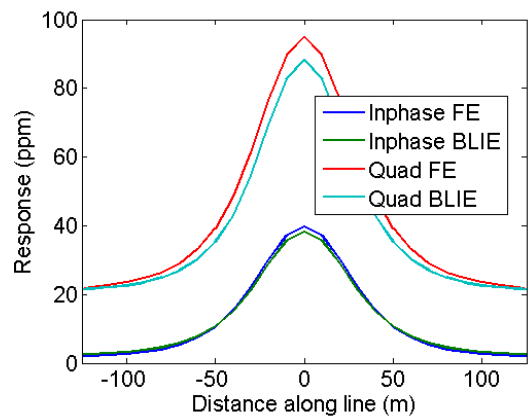

Figure 2. Comparison of the FE method and the high contrast IE method of Farquharson (2006). Both the inphase and quadrature parts are in excellent agreement.

Inversion methodology

We previously introduced the concept of a moving sensitivity domain for 3D AEM inversion (Cox and Zhdanov, 2007; Cox et al. 2010, 2012). According to this concept, one only needs to calculate the responses and sensitivities for that part of the 3D earth model that is within the AEM system's footprint, and then superimpose the sensitivities for all sensitivity domains into a single, sparse sensitivity matrix for the entire 3D earth model. Our modeling was based on the 3D contraction IE method (Hursán and Zhdanov, 2002). For 3D AEM inversion with

DOI http://dx.doi.org/10.1190/segam2014-0927.1

the FE method, we preserve the moving sensitivity domain methodology and re-weighted regularized conjugate gradient (RRCG) method as described by Zhdanov (2002) and Cox et al. (2010). However, we have replaced the IE method for computing the fields and sensitivities with the FE method introduced above.

Every voxel in the inversion domain is of equal size in the x direction and the y direction (Figure 3). The larger cells of the variable conductivity domain are composed by averaging multiple cells. The sensitivities are computed only in the sensitivity domain for each sounding location. These are used to compute the descent direction in the conjugate gradient method. The uniform horizontal discretization prevents the need for resampling of the sensitivities. However, the forward modeling includes the variable conductivity domain, so the residuals are calculated using a larger domain than the sensitivities. This allows large contrast features which may be outside of the original sensitivity domain to be properly accounted for in the inversion.

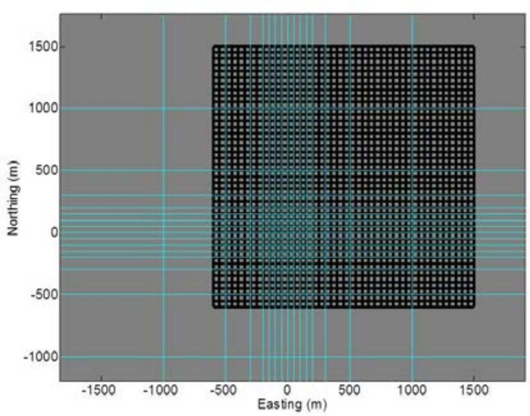

Figure 3: Illustration of inversion domain with a modeling mesh overlain. The black grid illustrates the inversion domain. The blue lines indicate the mesh location for a transmitter-receiver pair centered at (0,0). The blue mesh (modeling) will shift laterally relative to the black mesh (inversion) as the transmitter-receiver location changes.

Case study: Reid-Mahaffy test site, Ontario

The Reid-Mahaffy test site is located in the Abitibi Subprovince, immediately east of the Mattagami River Fault. The area is underlain by Archean (about 2.7 b.a.) mafic to intermediate metavolcanic rocks in the south, and felsic to intermediate metavolcanic rocks in the north, with a roughly EW-striking stratigraphy. The world-class Kidd Creek VMS deposit occurs to the southeast of the test site (Ontario Geological Survey, 2000). Drill holes within the test site were targeting conductive targets, and encountered massive sulfides and graphite with minor copper and zinc mineralization.

Many different airborne systems have been test in this area, including the DIGHEM frequency domain system, which is the focus of this paper. The DIGHEM system was configured with five operating frequencies: 868, 7025, and 56374 Hz horizontal coplanar and 1068 and 4820 Hz vertical coaxial. The transmitter-receiver separation was 6.3 m for the highest frequency and 8.0 m for the remainder. The survey was flown with a nominal bird height of approximately 32 m. The DIGHEM data were inverted for a 3D conductivity model with elements that were 20 m in the in-line direction and 25 m in the cross-line direction, and varied from 5 m to 20 m in the vertical direction. The model had a total depth of 160 m. The sensitivity domain of the DIGHEM system was set at 280 m. The 3D inversion for the DIGHEM data converged to a final misfit of 5% from an initial misfit of 70%. Figure 4 is an example of the conductivity model recovered from the 3D inversion.

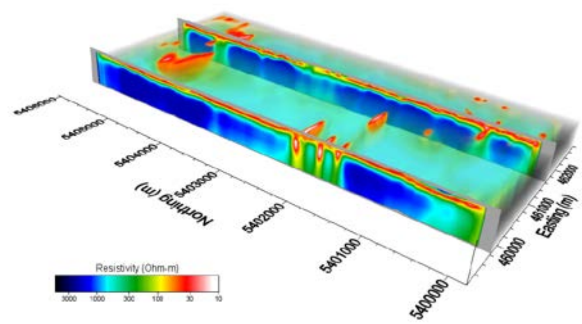

Figure 2: Perspective view of FE inversion results. The conductive overburden has been removed from the semi-transparent volume, but is shown on the cross-sections.

AEM data from the Reid-Mahaffy test site have previously been interpreted using a variety of 1D AEM methods (e.g., Witherly et al., 2004; Sattel, 2005; Vallee and Smith, 2007, 2009), as well as 3D inversion from Cox et al (2010). Figure 5 compares the inversion results from Cox et. al. (2010), which were based on the full integral equation method, and current results from the FE method. The results are shown along line 40, which is directly over three vertical conductors. Both methods used the same inversion parameters (regularization, weighting, etc.) and the same 100 Ohm-m starting model.

Overall, the two results are very similar. Both show conductive overburden between 20 Ohm-m and 50 Ohm-m, and both show 3 vertical conductors in the correct location as determined by drill holes. The hybrid solution shows a higher contrast and better defined edges of the conductors. It also shows somewhat thinner and more conductive

DOI http://dx.doi.org/10.1190/segam2014-0927.1

overburden. However, the FE method took 7 hours to complete the inversion, while the full IE method took 45 minutes.

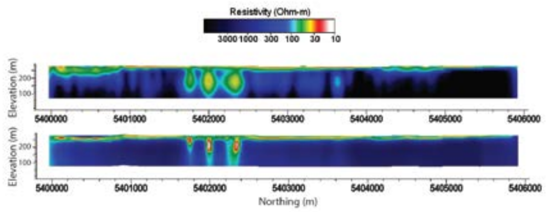

Figure 3: Comparison of IE and FE inversion results along line 40. The IE results are shown in the top panel, and the FE results are shown in the bottom panel.

The data fit for the FE inversion along line 40 is shown in Figure 6. For clarity, only the real part of the data is shown. The conductors clearly respond most strongly in the coaxial components, as should be expected for vertical structures. The low frequency coaxial channel (bottom blue line) shows significant noise, but the inversion is shown to be robust in the presence of this noise—fitting obvious signal but rejecting the noise.

For completeness, we compare these two inversion results to previous methods as compiled by Sattel (2005). Figure 7 shows various interpretation and inversion methods from other authors. The approximate inversion methods and transforms (EMFlow, Differential resistivity, Sengpiel's method, and Zohdy's method) show indications of the three conductors, but have significant artifacts. The 1D methods (1D Occam and 3 and 4 layered earth inversions) do not show the conductors.

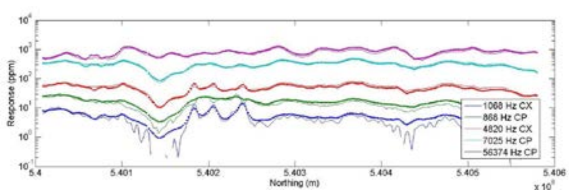

Figure 4: Data fit along line 30. The observed data is shown as the solid lines, and the predicted data is shown as the broken line. Only the real part of the data is shown.

Conclusions

We have presented a practical method of 3D AEM inversion that is suited to arbitrarily complex earth models with very high conductivity contrasts. The method is based on a hybrid edge-based FE-IE algorithm of forward modeling and regularized inversion with moving sensitivity domain.

The case study presents a 3D inversion of 90 line km of DIGHEM data from the Reid-Mahaffy test site. We show that the inversion results based on a hybrid FE-IE method are comparable to our previous 3D inversion produced by the integral equation method. The recovered contrast is higher and the boundaries are sharper with the FE-IE method, but the inversion took 10 times longer. Future research will be focused on application of this method to the 3D inversion of AEM surveys with rugged topography and high conductivity contrasts.

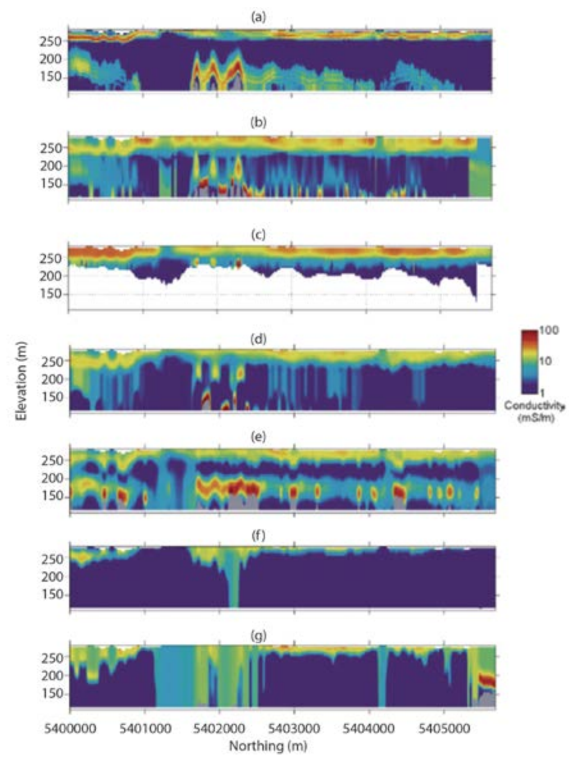

Figure 5: Vertical slice of line 40 from various approximate inversions, transforms, and 1D inversions from Sattel (2005). The methods used for the interpretation are (a) EMFlow, (b) Differential Resistivity, (c) Sengpiel's method, (d) Zohdy's method

Acknowledgements

The authors acknowledge the support of the University of Utah Consortium for Electromagnetic Modeling and Inversion (CEMI), and TechnoImaging.

DOI http://dx.doi.org/10.1190/segam2014-0927.1

http://dx.doi.org/10.1190/segam2014-0927.1

EDITED REFERENCES

Note: This reference list is a copy-edited version of the reference list submitted by the author. Reference lists for the 2014 SEG Technical Program Expanded Abstracts have been copy edited so that references provided with the online metadata for each paper will achieve a high degree of linking to cited sources that appear on the Web.

REFERENCES

Cox, L. H., G. A. Wilson, and M. S. Zhdanov, 2010, 3D inversion of airborne electromagnetic data using a moving footprint: Exploration Geophysics, **41**, no. 4, 250–259, http://dx.doi.org/10.1071/EG10003.

Cox, L. H., G. A. Wilson, and M. S. Zhdanov, 2012, 3D inversion of airborne electromagnetic data: Geophysics, **77**, no. 4, WB59–WB69, http://dx.doi.org/10.1190/geo2011-0370.1.

Cox, L. H., and M. S. Zhdanov, 2007, Large-scale 3D inversion of HEM data using a moving footprint: 77th Annual International Meeting, SEG, Expanded Abstracts, 467–470.

Ellis, R. G., 1999, Joint 3D electromagnetic inversion, *in* M. Oristaglio, and B. Spies, eds., Three-dimensional electromagnetics: SEG, 179–192.

Farquharson, C. G., K. Duckworth, and D. W. Oldenburg, 2006, Comparison of integral equation and physical scale modeling of the electromagnetic responses of models with large conductivity contrasts: Geophysics, **71**, no. 4, G169–G177, http://dx.doi.org/10.1190/1.2210847.

Gupta, P. K., A. P. Raiche, and F. Sugeng, 1989, Three-dimensional time-domain electromagnetic modelling using a compact finite-element frequency-stepping method: Geophysical Journal International, **96**, no. 3, 457–468, http://dx.doi.org/10.1111/j.1365-246X.1989.tb06007.x.

Hursán, G., and M. S. Zhdanov, 2002, Contraction integral equation method in three-dimensional electromagnetic modeling: Radio Science, **37**, no. 6, 1-1–1-13, http://dx.doi.org/10.1029/2001RS002513.

Mur, G., 1994, Edge elements, their advantages and their disadvantages: IEEE Transactions on Magnetics, **30**, no. 5, 3552–3557, http://dx.doi.org/10.1109/20.312706.

Ontario Geological Survey, 2000, Airborne magnetic and electromagnetic surveys, Reid-Mahaffy airborne geophysical test site survey: Ontario Geological Survey, Miscellaneous Release Data (MRD)-55.

Raiche, A., 1998, Modeling the time-domain response of AEM systems: Exploration Geophysics, **29**, no. 2, 103–106, http://dx.doi.org/10.1071/EG998103.

Raiche, A., and F. Sugeng, 1989, Predicting the transient EM response of complex structures using the compact finite-element method: Exploration Geophysics, **20**, no. 2, 51–55, http://dx.doi.org/10.1071/EG989051.

Raiche, A., F. Sugeng, and G. Wilson, 2007, Practical 3D EM inversion — P223F software suite: Presented at the 19th Geophysical Conference and Exhibition, ASEG.

Sattel, D., 2005, Inverting airborne electromagnetic data with Zohdy's method: Geophysics, **70**, no. 4, G77–G85.

Silvester, P. P., and R. L. Ferrari, 1996, Finite elements for electrical engineers, 3rd ed.: Cambridge University Press.

Sugeng, F., 1998, Modeling the 3D TDEM response using the 3D full-domain finite-element method based on the hexahedral edge-element technique: Exploration Geophysics, **29**, no. 4, 615–619, http://dx.doi.org/10.1071/EG998615.

Sugeng, F., and A. Raiche, 2004, Modelling the electromagnetic response in complex geological structures using the 3D finite-element method based on the hexahedral and the tetrahedral edge-element technique: Presented at the 17th Geophysical Conference and Exhibition, ASEG.

Vallée, M., and R. Smith, 2007, Comparison of fixed-wing airborne electromagnetic 1D inversion methods: Proceedings of Exploration 07: 5th Decennial International Conference on Mineral Exploration, 1067–1072.

Vallée, M., and R. Smith, 2009, Application of Occam's inversion to airborne time-domain electromagnetics: The Leading Edge, **28**, 284–287, http://dx.doi.org/10.1190/1.3104071.

Witherly, K., R. Irvine, and E. Morrison, 2004, The Geotech VTEM time-domain helicopter EM system: Presented at the 17th Geophysical Conference and Exhibition, ASEG.

Zhdanov, M. S., 2002, Geophysical inverse theory and regularization problems: Elsevier.

Zhdanov, M. S., 2009, Geophysical electromagnetic theory and methods: Elsevier.